Projective Invariants for Planar Contour Recognition*

Marc Van Diest, Luc Van Gool, Theo Moons** and Eric Pauwels**

Katholieke Universiteit Leuven, ESAT-MI2,
Kardinaal Mercierlaan 94, B-3001 LEUVEN, Belgium
e-mail: Luc.VanGool@esat.kuleuven.ac.be

Abstract. Implementation results for projective invariant descriptions of planar curves are presented. The paper outlines methods for the generation of projectively invariant representations of curve segments between bitangent points as well as – and this for the first time – segments between inflections. Their usefulness for recognition is illustrated. The semi-local nature of the invariant descriptions allows recognition of objects irrespective of overlap and other image degradations.

1 Projective, semi-differential invariants

For recognition of plane contours from arbitrary perspective views, projectively invariant descriptions can be used. Trying to minimize the efforts of calculating robust estimates for derivatives (as with differential invariants [5]) and reducing the dependence on finding points for a basis [6], *semi-differential invariant* descriptions were proposed [1, 3, 4]. These invariants need fewer points than required for a basis and lower order derivatives than needed for the differential invariants. The use of these semi-differential invariants for the recognition of planar, overlapping objects is demonstrated.

In the sequel, contour point coordinates $(x, y)^T$ will be written $\mathbf{x}$. Subscripts are used to denote fixed reference points, whereas superscripts will be used for the specification of the order of differentiation in the case of derivatives. Vertical bars indicate determinants.

2 Semi-local, projectively invariant descriptions

Two new semi-local schemes for the generation of projectively invariant curve descriptions are discussed, one for segments between bitangent point pairs, the other for segments between inflections, i.e. segments between points that are projectively invariant.

* The support of the Esprit project BRA EP 6448 "VIVA" and of the FKFO project 2.0065.90 is gratefully acknowledged.

** Theo Moons and Eric Pauwels gratefully acknowledge postdoctoral research grants of the Belgian National Fund for Scientific Research (N.F.W.O.).

Lecture Notes in Computer Science, Vol. 800
Jan-Olof Eklundh (Ed.)
Computer Vision – ECCV '94

2.1 Segments between bitangent points

Since inflections are rather unstable points to extract, and since bitangent points and tangent lines at inflections can be extracted with higher robustness, it is natural to preferentially look for descriptions based on such points and lines. Consider fig. 1. First, the bitangent points $\mathbf{b}_1$ and $\mathbf{b}_2$ and the intersection $\mathbf{c}$ of

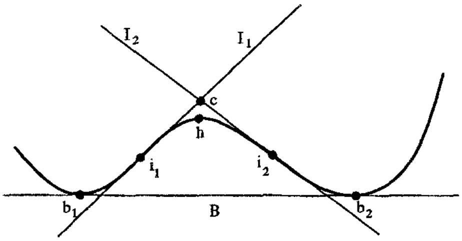

Fig. 1. Bitangent points and tangent lines at inflections can be extracted with sufficient robustness for them to be used as the basis of a projectively invariant, semi-local shape description.

the two tangent lines in the inflections are used to find a new invariant point on the contour, which lies between the inflections $\mathbf{i}_1$ and $\mathbf{i}_2$. This is achieved by calculating an invariant parameterization of the segment between the inflections using the semi-differential, invariant parameter

$$\int \mathrm{abs}\left(\frac{|\mathbf{x}-\mathbf{c}\ \ \mathbf{x}^{(1)}|}{|\mathbf{x}-\mathbf{b}_1\ \ \mathbf{x}-\mathbf{b}_2|^2}\right) dt \ . \tag{1}$$

This parameter is not truly invariant, but will only differ up to some factor between views. Normalizing the "length" between the inflections to 1 this caveat can be lifted. At the point where the parameter reaches value $\frac{1}{2}$, a new invariant contour point is found, which will be referred to as $\mathbf{h}$. Now it might seem that the inflections have been reintroduced, and hence also the vulnerability to errors in their position. This is not the case though. The above integral changes very slowly in the neighbourhood of the inflections, since the area between the curve and the tangent line is very small there. Thus, even if the inflections are ill-placed, the resulting error in the invariant parameter will be limited.

Having found the new invariant point $\mathbf{h}$, an invariant signature is built for the contour segments on either side of it. At this stage, four invariant points are known, which could be used as a projective frame: $\mathbf{b}_1, \mathbf{b}_2, \mathbf{c}$, and $\mathbf{h}$. Together with any other point of the segment, they yield two independent 5-point cross-ratios. However, an alternative strategy can be used, which yields an invariant as a function of an invariant parameter, thereby making explicit the correspondences between points in different views (these should have the same parameter value).

As a (relative) invariant parameter

$$\int \text{abs}\left(\frac{|\mathbf{x}-\mathbf{b}_2\ \ \mathbf{x}^{(1)}|}{|\mathbf{x}-\mathbf{b}_2\ \ \mathbf{x}-\mathbf{c}|^2}\right) dt \tag{2}$$

is used for the first half (the part between $\mathbf{b}_1$ and $\mathbf{h}$). The parameter for the second half between $\mathbf{h}$ and $\mathbf{b}_2$ is exactly the same, but with $\mathbf{b}_1$ replacing $\mathbf{b}_2$. Again, both lengths have to be normalized to 1 in order to eliminate a factor. In summary then, the parameter will go from -1 to 1, with the parameter value at $\mathbf{h}$ being 0.

In order to obtain an invariant signature, a second, independent invariant is required. For the points with parameter values in the range $[-1, 0]$

$$\frac{|\mathbf{x}-\mathbf{c}\ \ \mathbf{x}-\mathbf{b}_1|}{|\mathbf{x}-\mathbf{c}\ \ \mathbf{x}-\mathbf{b}_2|} \tag{3}$$

is used, whereas for the points with parameter values in the range $[0, 1]$ a similar expression is used, but with $\mathbf{b}_1$ and $\mathbf{b}_2$ swapped.

This construction results in a representation as the one shown in fig. 2. On the abscissa the parameter is used, whereas the last mentioned invariant is used for the ordinate values. Rather than matching such a complete invariant signature, a few invariant numbers are used. These are the ordinate values read out at the parameter values -0.9, -0.25, 0.25 and 0.9.

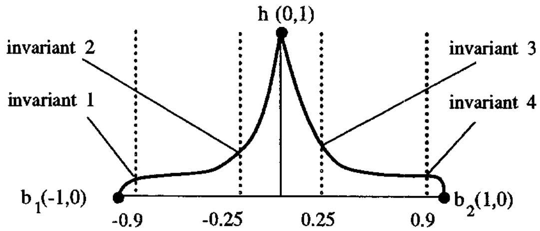

Fig. 2. Canonical frame and invariants for segments between bitangent points.

In addition to the forementioned invariants, a cross-ratio can be calculated which does not require any information beyond that available after the very first stage: the bitangent line and the tangent lines at the inflections. These tangent lines will intersect the bitangent line in two points, which taken together with the bitangent points yield 4 collinear points. Their cross-ratio and the four other invariants were combined in a 5-component feature vector.

2.2 Segments between inflections

Although more difficult to extract precisely, segments between inflections may be used when no bitangent segments are available, e.g. due to occlusion. In a similar vein as with the previous method, the generation of an invariant representation for such segments is initiated by the extraction of the line connecting the inflections and the tangent lines at the inflections. In a sense, the bitangent line is replaced by the line joining the inflections. However, the further constructions described earlier would fail. Instead, the projective invariance of a bundle of conics is used. The construction yields an additional invariant point on the curve. The two inflections, the intersection of the lines tangent at the inflections and that additional point together fix a projective frame. Although the method propounded here succinctly has a constructive flavour, there are purely semi-differential strategies to find an additional point.

The bundle of conic sections is defined by three lines: the line connecting the inflections and the two lines tangent at the inflections. The first line taken twice and the latter pair of lines each constitute a degenerate conic. The bundle is then defined as

$$\lambda\left(m_1x+n_1y+o_1\right)^2+\left(m_2x+n_2y+o_2\right)\left(m_3x+n_3y+o_3\right)=0\ , \qquad (4)$$

where λ is an arbitary real number and the linear expressions in x and y are the equations for the lines. From this bundle of conic sections, the one with the most negative λ that touches the contour is taken. The point where it touches the contour is the fourth point. Fixing the positions of the four points creates the projective frame. In the sequel, the frame will be defined with the coordinates of the two inflections at $(-1,0)$ and $(1,0)$, those of the tangents intersection at $(0,3)$ and those of the newly found point at $(0,1)$. This yields a representation as shown in fig. 3.

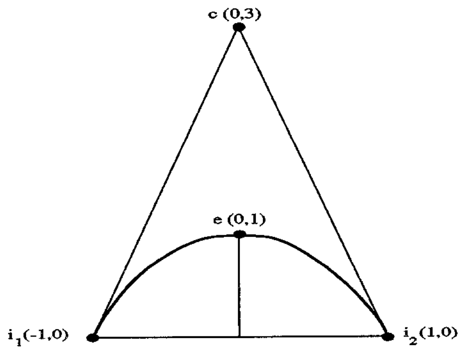

Fig. 3. Projectively invariant representation for segments between inflections.

As before, rather than matching complete signatures, recognition as reported here is based on the extraction of invariant numbers. In fact only the ratio of curvatures at the point where the selected ellipse touches the curve, was used. This ratio of the curve's curvature over the ellipse's curvature is a projective invariant [2].

3 Object recognition

The use of the invariant representation methods for segments between bitangent points and inflections are now illustrated. As a test case, consider the scene of fig. 4. Model descriptions and the corresponding invariant numbers for the different segments were extracted from separate views of the three objects. The invariants were used to generate a feature vector. Each segment in fig. 4 was considered to match the segment from the models with the nearest feature vector. The distance between test segment a and model segment b was obtained as

$$D_{\mathbf{a},\mathbf{b}} = \sum_{i=1}^{N} \frac{|f_{\mathbf{a}i} - f_{\mathbf{b}i}|}{\sigma_i} \quad , \tag{5}$$

where σ_i is the standard deviation for feature f_i calculated over all segments in the models and N is the number of features. All segments in the image that corresponded to a true model segment, were used in the experiment. The numbers

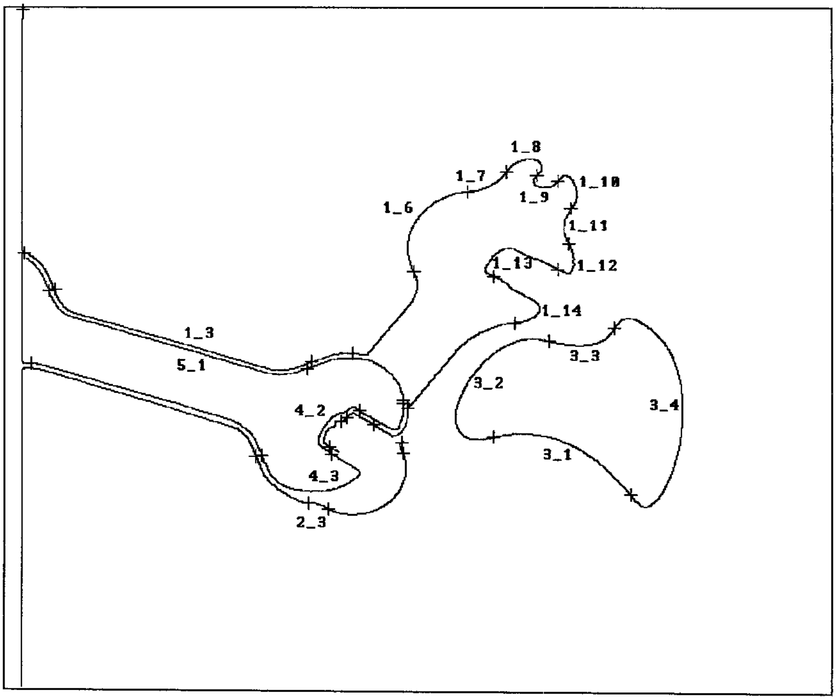

Fig. 4. Numbered edge segments extracted from test scene.

in fig. 4 are assigned to segments between two neighbouring inflections. For the bitangent construction, these segments have to be thought as being extended on either side up to the next pair of bitangent points. In fact, this extension is not always possible, but we will introduce next a slightly modified type of bitangent segment, making this extension more general.

Overlap together with erroneous edge detection may drastically reduce the number of bitangent segments that can correctly be extracted. Moreover, the largest and therefore best suited segments often are the most vulnerable. Therefore, some additional segments were included in the "bitangent" approach, obtained by extending a segment to the next inflection on one side and an opposite tangent point on the other side, obtained by rotating a line about that inflection. Such segments are illustrated in fig. 5. They allow for the same constructions as

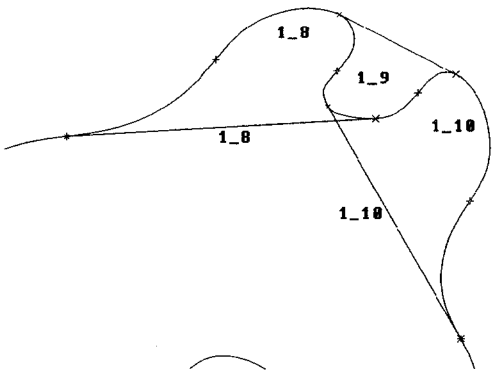

Fig. 5. Examples of pseudo-bitangent segments: the line labeled 1-8 connects an inflection and the corresponding tangent point, delimiting the extended segment 1-8. Similarly, such segment was obtained between the points connected by the line 1-10.

the bitangent segments and will be referred to as "pseudo-bitangent" segments. Bitangent segments are preferred due to higher robustness.

Before discussing the matching results, the invariant representations for the segments 1-8 and 1-9 from fig. 4 are illustrated. Segment 1-9 can be extended to a bitangent segment, whereas segment 1-8 is extended to a pseudo-bitangent segment, as shown in fig. 5. The invariant descriptions obtained using the between-bitangents and between-inflections methods are shown in fig. 6, both for the test scene and for the model. As can be seen from these figures, the distinction between the segments (1-8 continuous, 1-9 dotted line) is possible from such invariant descriptions. Although in this case the construction between inflections performs well compared to the bitangent method, it is fair to say that the bitangent method performs typically better, whereas the average performance of the inflection method is worse than that shown here.

Hence, the recognition procedure is planned to start with the analysis of bitangent and pseudo-bitangent segments. Table 1 summarizes the results for the bitangent constructions. The table contains the distance based rank-order of the correct model segment. The first row gives the number of the segment in

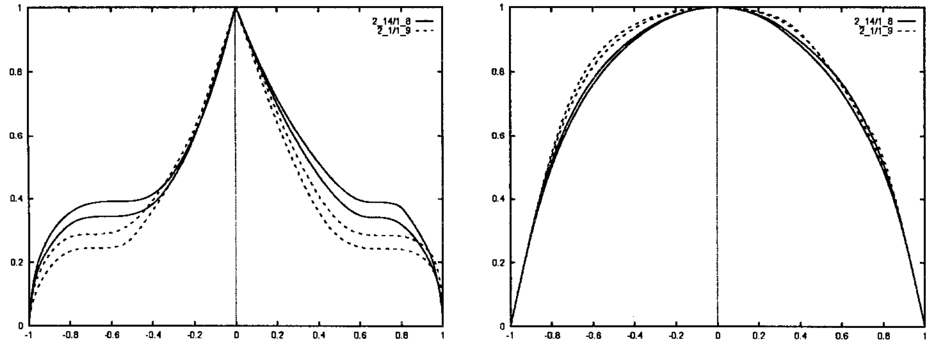

Fig. 6. Left: illustration of the bitangent construction for test scene and model for segments 1-8 and 1-9. Right: their between-inflections representations.

Table 1. Rank order of the correct model segment in the list of sorted distances to the model segments. "1" means that the correct segment is the best guess, "2" that the correct segment is the second best guess, etc.

segment nmb	1-6	1-7	1-8	1-9	1-10	1-11	1-12	1-13	2-3	3-1	3-3	4-2
class. rank	1	1	1	2	1	2	1	12	2	1	1	4

fig. 4. Only segments for which a bitangent or pseudo-bitangent extension was possible, are listed. It are these *extended* segments the table refers to.

Both the definition of the distance and the classification method *per se* have been kept extremely simple in this test. The performance is expected to improve when more elaborate statistics are invoked. Results were found to be comparable to those obtained with a selection of invariants extracted from the 5-point construction [6]. For this case, the latter had the correct model segment 6 times at first position. Lumping all features together in a single feature vector kept the hit rate at 7 (same as the proposed bitangent method). Yet, in 9 out of 12 cases either the proposed method or the 5-point method had the correct model segment at first position.

The method that works on segments between inflections is considered a fall-back solution, rather than a first-line approach. Looking at the test image (fig. 4), the risk of not being able to extract a bitangent or pseudo-bitangent segment for the leftmost spanner is real. Everything hinges on the extraction of the bitangent segment around 4-2. Knowing the state-of-the-art in edge detection, one can hardly expect to be always as fortunate as in this case. The unextended segment 1-3 (i.e. the segment between the inflections) might be called upon then, using the construction between neighbouring inflections. The resulting ratio of curvatures is shown in table 2, together with three more examples. The discriminant power of this invariant is rather low.

Table 2. Values of the curvature ratio for the different segments in the reference image.

segment nmb	curv. ratio ref.	curv. ratio test
1-3	0.0636	0.0560
1-6	0.8632	0.8417
1-7	0.8495	0.8588
1-8	0.5592	0.5704

4 Conclusions

Novel methods for the generation of projectively invariant descriptions for plane curve segments were devised and illustrated.

One of the approaches was aimed at segments between bitangent points and can be considered to take on a role complementary to that of the 5-point cross ratio based method. The idea is to build a recognition system that is opportunistic in that it uses several constructions simultaneously, and selects promising segments through a kind of voting mechanism.

The other approach was designed for segments between inflections. Although this method lacks the discriminant power of the bitangent methods, it can nevertheless be crucial as a last resort, when all bitangent segments are occluded or their edges noisy or incomplete. It should be added that the inclusion of additional measurements from these invariant descriptions is expected to improve the performance of this method. In contrast to the bitangent methods, the current implementation works with the ratio of curvatures as the only invariant.

References

1. M. Brill, E. Barrett, and P. Payton, Projective invariants for curves in two and three dimensions, chapter 9 in *Applications of invariance in vision*, Eds. J. Mundy and A. Zisserman, pp. 193-214, MIT Press, 1992
2. M. Van Diest, L. Van Gool, T. Moons, and E. Pauwels, Projective invariants for planar contour recognition, Techn. Report KUL/ESAT/MI2/9305, 1993
3. L. Van Gool, P. Kempenaers, and A. Oosterlinck, Recognition and semi-differential invariants, *IEEE Conf. on Computer Vision and Pattern Recognition*, pp.454-460, 1991
4. L. Van Gool, T. Moons, E. Pauwels, and A. Oosterlinck, Semi-differential invariants, chapter 8 in *Applications of invariance in vision*, Eds. J. Mundy and A. Zisserman, pp. 157-192, MIT Press, 1992
5. I. Weiss, Noise resistant invariants of curves, in *Applications of invariance in vision*, Eds. J. Mundy and A. Zisserman, pp. 135-156, MIT Press, 1992
6. A. Zisserman, D. Forsyth, J. Mundy, C. Rothwell, Recognizing general curved objects efficiently, in *Applications of invariance in vision*, Eds. J. Mundy and A. Zisserman, pp. 228-251, MIT Press, 1992